ELSEVIER

Journal of Hazardous Materials 38 (1994) 163–185

JOURNAL OF HAZARDOUS MATERIALS

Dispersive–convective characteristics in the biorestoration of contaminated soil with a heterogeneous formation

Xiaoqing Yang, L.E. Erickson*, L.T. Fan

Department of Chemical Engineering, Durland Hall, Kansas State University, Manhattan, KS 66506-5102, USA

Received 31 August 1993; accepted in revised form 20 January 1994

Abstract

A hydrochemical model comprising a set of coupled partial differential equations has been proposed for the bioremediation of contaminated soil with a heterogeneous formation. The soil bed is a layer of water-saturated porous medium with dominant bypassing flow. Inside the layer, the groundwater flow is relatively slow such that the magnitudes of convection and dispersion are of the same order. This model describes, both spatially and temporally, the contaminant fate, microorganism growth and oxygen consumption. The results of simulation indicate that the velocity of the groundwater flow affects significantly the rate of contaminant depletion; the higher the velocity, the greater the availability of oxygen and the faster the substrate consumption. When the velocity is low, an anaerobic zone is generated in the clay layer, thereby rendering the biodegradation rate oxygen limited and, in turn, prolonging the remediation time.

1. Introduction

Biological restoration of soils contaminated with organic chemicals is an innovative treatment technology that can often meet the goal of achieving a permanent clean-up remedy with minimal environmental impact. Appreciation of the rate of contaminant attenuation in soil is necessary for successful design. Soils often exhibit a variety of heterogeneities, such as rock fractures, drying clay cracks and clay mounds. A commonly encountered soil is the so-called "structured soil" containing relatively large and essentially continuous voids [1]. Soil aggregates formed from fine particles usually retard flow inside [2–4]. Numerous aquifers contain layers of silt and clay; this results in field-scale variability in hydraulic properties. Such hydraulic heterogeneities

* Corresponding author. Tel.: 913-532-5584. Fax: 913-532-7372.

SSDI 0304-3894(94)00011-5

may create macroscopically nonuniform flow fields with widely different velocities, often referred to as preferential flows or bypassing phenomena [5].

Information on water flow in subsurface systems provided by modeling or field measurements is essential to the study of bioremediation. Microscopic differences in structure, flow and transport in heterogeneous soils are frequently described using dual-porosity models which assume that the medium consists of two types of voids, one associated with the fracture network and the other with a less permeable pore system within the aggregates [4, 6–8]. Two-domain models or compartment models have been suggested to represent the macroscopic structure [9–12]. These models assume that hydraulic properties in each domain or compartment are unique and different from those in the other.

In the past few years, a number of investigators have developed models or carried out experiments that provide insight into the rate-limiting processes of bioremediation, such as microbial growth, contaminant depletion and nutrient uptake [13–19]. Dhawan et al. [20] have simulated the transport and biodegradation of a contaminant inside soil aggregates where microorganisms assimilate the substrate in the liquid and consume the dissolved oxygen. Emphasizing the inaccessibility of microorganisms to the inside of very small aggregates, Chung et al. [21] have discussed whether biodegradation may be kinetically limited by intraparticle diffusion. Little attention has been focused on the contaminant fate in a soil with variably permeable layers. Current literature does not contain sufficient information on the influence of a layer with both much lower permeability than its surroundings and a very slow or no convective flow in it.

The objective of the present work is to propose a mathematical model accounting for microbial growth and biodegradation in a region of the aquifer with low hydraulic conductivity and extensive bypassing flow. The adsorption–desorption and depletion of the contaminant or substrate are simulated numerically to analyze the biochemical processes under conditions where groundwater flow is extremely slow, and thus transport by convection and dispersion is of the same order of magnitude. The importance of such a region to the whole process of bioremediation is then discussed.

2. Model development

The system to be modeled involves transport and biodegradation of the contaminant in a saturated subsurface soil with a layer where the flow is very slow and is accompanied by extensive bypassing. The soil under consideration is schematically illustrated in Fig. 1. The heterogeneity is characterized by the very large bypassing flow rate F_β, and the very small flow rate F_α, through the low permeability region. The region is also surrounded by two chambers of high permeability, which link the region with the outside flow. The bioremediation in the soil is an aerobic process of contaminant depletion, oxygen consumption, and microbial growth. The model describing the transport and biodegradation is derived based on the following assumptions.

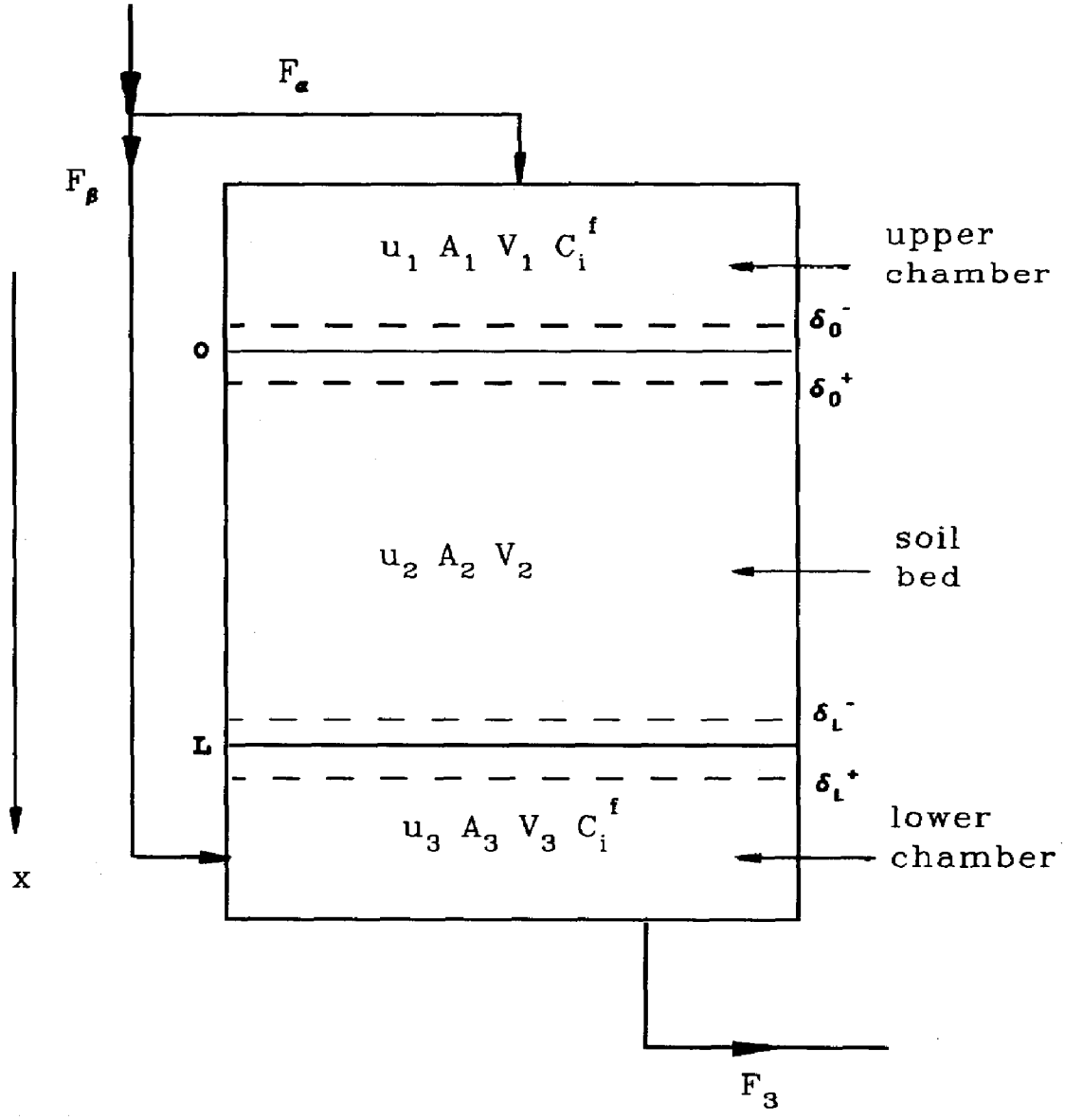

Fig. 1. Schematic diagram of the system: the upper and lower chambers are regions of high permeability while the portion of the soil bed from 0 to L is the region of low permeability.

1. The system comprises continuous media, i.e., the microscopic movement, and reaction in pores may be averaged over a sufficiently large volume of the medium to obtain a macroscopic description of the state variables.
2. The region of interest is saturated, homogeneous and isotropic.
3. A one-dimensional flow governed by Darcy's law prevails.
4. The concentration of microorganisms or biomass attached to the soil surface and that in the suspension are related through a partition coefficient.

5. The reaction rate follows the Monod kinetic model and depends only on the concentrations of the three components: oxygen, biomass, and substrate (contaminant).
6. The concentration driving force governs the net rate of transport of the contaminant from the solid surface into the liquid phase.

Under these assumptions, a mass balance over the liquid phase gives the governing equation of the ith species:

$$\frac{\partial(\varepsilon C_i)}{\partial t} = -\frac{\partial(u\varepsilon C_i)}{\partial x} + \frac{\partial}{\partial x}\left(\varepsilon E_i \frac{\partial C_i}{\partial x}\right) + G_i, \tag{1}$$

where C_i is the concentration of the ith species in the liquid phase, with the subscripts, $i = \mathrm{s}, \mathrm{o}, \mathrm{b}$, referring to substrate, oxygen, and biomass, respectively, t the time, x the axial position, u the mean pore water velocity, ε the void fraction of soil, E_i the dispersion coefficient, and G_i the rate of mass generation.

It is assumed that E_i reflects two additive phenomena, i.e., ionic or molecular diffusion arising from the thermal motion of dissolved constituents and hydrodynamic dispersion resulting from the local deviation from the average fluid flux. Generally, the hydrodynamic dispersion is dominant in a convective flow. Since the aqueous diffusion coefficients for many hydrocarbons and oxygen are of the same order of magnitude, the dispersion coefficients of different species are considered to be identical in this work. Cussler [22] has shown how the Peclet number varies with the particle Reynolds number in porous media.

The actual microbial movement in subsurface soils is very complicated because of the interplay of the native motion of cells, guided by the local physicochemical environment, adsorption, filtration, and convection of cells within the flow. Most eucaryotic and procaryotic cells are mobile by means of flagella, and a type of eucaryotic cell has a locomotive organ as celia, while a few types of bacteria possess a gliding motion that allows them to move over surfaces by an unknown mechanism [23]. Matthess et al. [24] have further studied the sorption, filtration, convection, and dispersion of bacteria and viruses in groundwater. The review paper of Baveye and Valocchi [25] divides the current investigations on the transport of biological reacting solutes into three major conceptual frameworks constructed on the assumptions of continuous uniform biofilm, discrete attached microcolonies, and partitioning of floating cells and fixed groups. Studies based on the first two assumptions usually emphasize the fate of the organic chemicals and neglect the influence of microbial concentration and/or microbial movement [26–29]. Models based on the partitioning assumption consider the microbial movement in aqueous phase as dispersive–convective, while the concentration of the surface-attached microorganisms and that of the floating groups are at instantaneous equilibrium and related by a partition coefficient [18, 20, 30]. The present model also follows this rationale.

Complete degradation of organic chemicals to carbon dioxide and water depends on the complex interplay between many microbial species. Numerous metabolic pathways involved in the decomposition of organic chemicals have been proposed [31, 32]; nevertheless, the knowledge of the pathways is far from complete due to the

complexities of indigenous microbial communities and the growing media in soils. The depletion of organic carbon and the growth of microorganisms are generally characterized by the following stoichiometric reaction:

$$CH_mO_l + aNH_3 + bO_2 \rightarrow yCH_pO_nN_q + zCH_rO_sN_t + cH_2O + dCO_2,$$

where CH_mO_l is the elemental composition of the organic chemical providing carbon and energy for microorganism growth, $CH_pO_nN_q$ is the simplified stoichiometric formula of the microorganisms, and $CH_rO_sN_t$ accounts for the extracellular products. The rate of the reaction is affected, however, not only by the concentrations of substrate and biomass, but also by the particular enzymes present, available nutrients, oxygen concentration in aerobic conditions, temperature and light. Monod kinetics usually serves to quantify the transformation rate:

$$-r_i = \frac{\mu_{mi}}{Y_i} R_b C_b \left(\frac{C_i}{K_{si} + C_i}\right) \Pi_j \left(\frac{C_j}{K_{sj} + C_j}\right), \tag{2}$$

where C_i is the carbon source concentration of the ith component, and C_j is the concentration (or intensity) of other rate-limiting substances [33].

The population of soil microorganisms is composed mainly of the surface-attached microcolonies, which also participate in the assimilation of organics in the liquid phase and are considered to constitute the concentration of biomass on the solid particles. Consequently, the total biomass concentration available for the liquid-phase reactions is $(C_b + \rho q_b/\varepsilon)$, in which q_b is the biomass concentration on the solid particles. A local equilibrium prevails between the biomass concentration of floating cells and that of attached ones, i.e., $q_b = K_{db} C_b$, where K_{db} is the partition coefficient. By introducing the retardation factor R_b, defined as

$$R_b = 1 + \frac{\rho K_{db}}{\varepsilon}, \tag{3}$$

the biomass concentration available for the liquid-phase reactions is $R_b C_b$. By considering the oxygen availability as the only growth limiting factor besides the substrate, the governing equation for biomass becomes

$$\frac{\partial (R_b C_b)}{\partial t} = \frac{\partial}{\partial x}\left(E \frac{\partial C_b}{\partial x}\right) - \frac{\partial (u C_b)}{\partial x} + \mu_m R_b C_b \left(\frac{C_s}{K_s + C_s}\right) \times \left(\frac{C_o}{K_o + C_o}\right) - k_d R_b C_b \tag{4}$$

where $k_d R_b C_b$ accounts for endogeneous metabolism and cell decay.

Since oxygen is not adsorbed on the solid particles, its governing equation is

$$\frac{\partial C_o}{\partial t} = \frac{\partial}{\partial x}\left(E \frac{\partial C_o}{\partial x}\right) - \frac{\partial (u C_o)}{\partial x} - \frac{\mu_m}{Y_o} R_b C_b \left(\frac{C_s}{K_s + C_s}\right)\left(\frac{C_o}{K_o + C_o}\right). \tag{5}$$

The solid phase of the soil comprises various constituents. The contaminant in the water solution may interact with these constituents at different rates and with different

intensities. Sorption or exchange reactions perceived as instantaneous are described by equilibrium isotherms which can be of a linear, Freundlich or Langmuir type, or can be of other functional forms [34, 35]. Review of the microscopic mechanisms of various sorption phenomena and the corresponding kinetic simulations can be found in [1, 36, 37].

The present work also resorts to a kinetic approach to represent the adsorption and desorption of the contaminant between the solid and liquid phases. By assuming that the substrate is homogeneously distributed on the surface of solid particles, the first-order rate expression attains the form

$$\rho \frac{\partial q_s}{\partial t} = -ak_s\left(\frac{q_s}{K_{ds}} - C_s\right). \tag{6}$$

A mass balance of substrate over the liquid phase gives the governing equation for substrate:

$$\frac{\partial C_s}{\partial t} = \frac{\partial}{\partial x}\left(E\frac{\partial C_s}{\partial x}\right) - \frac{\partial(uC_s)}{\partial x} + \frac{k_s a}{\varepsilon}\left(\frac{q_s}{K_{ds}} - C_s\right) - \frac{\mu_m}{Y_s}R_b C_b\left(\frac{C_s}{K_s + C_s}\right)\left(\frac{C_o}{K_o + C_o}\right). \tag{7}$$

The above two equations together with Darcy's law describing the relationship between the groundwater flow velocity and pressure head as well as the appropriate boundary and initial conditions constitute a mathematically closed model.

To investigate the heterogeneity of the system, the boundaries need be carefully defined, and the boundary conditions need be derived from the continuity of concentration and that of mass flux. A mass balance over the upper chamber is

$$V_1\left(\frac{\partial C_i}{\partial t}\right) = F_\alpha C_i^f - \left(u_1 A_1 C_i|_{x=0^-} - E_1 A_1 \left.\frac{\partial C_i}{\partial x}\right|_{x=0^-}\right) + V_1 r_i. \tag{8}$$

Complete mixing is assumed in the upper and lower chambers for the present model; therefore,

$$F_\alpha = u_1 A_1. \tag{9}$$

A mass balance over the upper interface control volume leads to

$$(\delta_0^- A_1 + \delta_0^+ A_2)\left(\frac{\partial C_i}{\partial t}\right) = \left[\left(u_1 A_1 C_i|_{x=\delta_0^-} - E_1 A_1 \left.\frac{\partial C_i}{\partial x}\right|_{x=\delta_0^-}\right) + \delta_0^- A_1 r_i\right] - \left[u_2 A_2 C_i|_{x=\delta_0^+} - E_2 A_2 \left.\frac{\partial C_i}{\partial x}\right|_{x=\delta_0^+}\right) + \delta_0^+ A_2 r_i\Bigg]. \tag{10}$$

As the width of the interface control volume vanishes, i.e., $\delta_0^- \to 0^-$ and $\delta_0^+ \to 0^+$, the above equation becomes

$$u_1 A_1 C_i|_{x=0^-} - E_1 A_1 \left.\frac{\partial C_i}{\partial x}\right|_{x=0^-} = u_2 A_2 C_i|_{x=0^+} - E_2 A_2 \left.\frac{\partial C_i}{\partial x}\right|_{x=0^+}. \tag{11}$$

Combining this equation with (8) and taking into account the flow rate continuity, i.e., $u_1A_1 = u_2A_2$, give rise to the upper boundary conditions

$$V_1\left(\frac{\partial C_i}{\partial t}\right) = u_2A_2C_i^f - \left(u_2A_2C_i|_{x=0^+} - E_2A_2\left.\frac{\partial C_i}{\partial x}\right|_{x=0^+}\right) + V_1r_i. \tag{12}$$

A mass balance over the lower chamber yields

$$V_3\left(\frac{\partial C_i}{\partial t}\right) = C_i^fF_\beta - C_iF_3 + \left(u_3A_3C_i|_{x=L^+} - E_3A_3\left.\frac{\partial C_i}{\partial x}\right|_{x=L^+}\right) + V_3r_i. \tag{13}$$

A mass balance over the lower interface control volume gives

$$(\delta_L^-A_2 + \delta_L^+A_3)\left(\frac{\partial C_i}{\partial t}\right) = \left[\left(u_2A_2C_i|_{x=L^-} - E_2A_2\left.\frac{\partial C_i}{\partial x}\right|_{x=L^-}\right) + \delta_L^-A_2r_i\right] - \left[\left(u_3A_3C_i|_{x=L^+} - E_3A_3\left.\frac{\partial C_i}{\partial x}\right|_{x=L^+}\right) + \delta_L^+A_3r_i\right]. \tag{14}$$

As $\delta_L^- \to 0$ and $\delta_L^+ \to 0$, this equation becomes

$$u_2A_2C_i|_{x=L^-} - E_2A_2\left.\frac{\partial C_i}{\partial x}\right|_{x=L^-} = u_3A_3C_i|_{x=L^+} - E_3A_3\left.\frac{\partial C_i}{\partial x}\right|_{x=L^+}. \tag{15}$$

Combining this equation with (13) and taking into account the flow rate continuity,

$$F_3 = F_\alpha + F_\beta, \tag{16}$$

yield the lower boundary conditions

$$V_3\left(\frac{\partial C_i}{\partial t}\right) = F_\beta(C_i^f - C_i) - u_2A_2C_i + \left(u_2A_2C_i|_{x=L^-} - E_2A_2\left.\frac{\partial C_i}{\partial x}\right|_{x=L^-}\right) + V_3r_3. \tag{17}$$

The flow rate F_β is considered to be much larger than the flow rate F_α, and $C_s^f = 0$; as a result, the reaction and accumulation terms in the upper and lower chambers are neglected. Furthermore, the concentration of every species in the lower chamber is approximately equal to the feed concentration due to the preferential bypass flow. Hence, the upper boundary conditions reduce to

$$C_i^f = C_i|_{x=0^+} - \left.\frac{E}{u}\frac{\partial C_i}{\partial x}\right|_{x=0^+} \tag{18}$$

and the lower boundary conditions reduce to

$$C_i^f = C_i|_{x=L^-} - \left.\frac{E}{u}\frac{\partial C_i}{\partial x}\right|_{x=L^-}. \tag{19}$$

These boundary conditions are appropriate for a very slow flow within the soil layer when bypass flow around it predominates. The outlet boundary condition is inad-

equate when the flow rate of bypassing is of equivalent magnitude with or smaller than that through the soil layer. The concentration of the ith species, C_i^f, outside the low permeability region is

$$C_s^f = 0, \qquad C_o^f = C_o^s, \qquad C_b^f = C_{b0}. \tag{20}$$

The initial conditions are

$$C_s = C_{so}^*, \qquad q_s = q_{so}, \qquad C_o = C_o^s, \qquad C_b = C_{b0}, \quad \text{at } t = 0,\ 0 < x < L, \tag{21}$$

where q_{so} is the initial concentration of substrate in the soil particle phase, C_{so}^* the concentration of substrate in the liquid phase which is in equilibrium with q_{so}, and C_o^s the saturated concentration of oxygen in the atmosphere.

Dimensionless variables are defined as follows:

$$\theta = tu/L, \qquad X = x/L, \qquad \bar{C}_s = C_s/C_{so}^*, \qquad \bar{C}_o = C_o/C_o^s,$$

$$\bar{C}_b = C_b/C_b^*, \qquad \bar{q}_s = q_s/q_{so}, \tag{22}$$

where $C_b^* = (q_{so}R_sY_s)/(K_{ds}R_b)$ is the maximum producible concentration of biomass from a substrate deposit in the bed. The governing equations may be written in terms of dimensionless variables and parameters; this yields

$$\frac{\partial \bar{C}_s}{\partial \theta} = \frac{1}{Pe}\frac{\partial^2 \bar{C}_s}{\partial X^2} - \frac{\partial \bar{C}_s}{\partial X} + Stm(\bar{q}_s - \bar{C}_s) - N_{r1}R_sR, \tag{23}$$

$$\frac{\partial \bar{C}_o}{\partial \theta} = \frac{1}{Pe}\frac{\partial^2 \bar{C}_o}{\partial X^2} - \frac{\partial \bar{C}_o}{\partial X} - N_{r1}WR, \tag{24}$$

$$\frac{\partial \bar{C}_b}{\partial \theta} = \frac{1}{R_bPe}\frac{\partial^2 \bar{C}_b}{\partial X^2} - \frac{1}{R_b}\frac{\partial \bar{C}_b}{\partial X} + N_{r1}R - N_{r2}\bar{C}_b, \tag{25}$$

$$\frac{\partial \bar{q}_s}{\partial \theta} = -\frac{Stm}{R_s - 1}(\bar{q}_s - \bar{C}_s). \tag{26}$$

In the above equations,

$$R = \bar{C}_b\left(\frac{\bar{C}_s}{\bar{K} + \bar{C}_s}\right)\left(\frac{\bar{C}_o}{\bar{K}_o + \bar{C}_o}\right), \tag{27}$$

$$\bar{K}_s = \frac{K_sK_{ds}}{q_{so}}, \tag{28}$$

$$\bar{K}_o = \frac{K_o}{C_o^s}, \tag{29}$$

$$Pe = \frac{Lu}{E}, \tag{30}$$

$$N_{r1} = \frac{\mu_m L}{u}, \tag{31}$$

$$N_{r2} = \frac{k_d L}{u}, \tag{32}$$

$$Stm = \frac{k_s a L}{\varepsilon u}, \tag{33}$$

$$R_s = 1 + \frac{\rho K_{ds}}{\varepsilon}, \tag{34}$$

$$W = \frac{C^*_{s0} R_s Y_s}{C^s_o Y_o}. \tag{35}$$

The dimensionless values of the variables are subject to change under different circumstances; however, it is possible to choose some characteristic values that would be feasible.

3. Numerical solution

The governing equations in the form of coupled nonlinear partial differential equations have been numerically solved by a finite difference algorithm [38]. Equations (23)–(26) can be compactly rewritten as

$$\frac{\partial \bar{C}_i}{\partial \theta} = P_{1,i} \frac{\partial^2 \bar{C}_i}{\partial X^2} - P_{2,i} \frac{\partial \bar{C}_i}{\partial X} + f_i. \tag{36}$$

The semi-implicit finite difference scheme for this equation has been constructed as

$$\begin{aligned} \frac{(\bar{C}_i)_j^{n+1} - (\bar{C}_i)_j^n}{\Delta\theta} = {} & P_{1,i}\left(\frac{(\bar{C}_i)_{j+1}^{n+1} - 2(\bar{C}_i)_j^{n+1} + (\bar{C}_i)_{j-1}^{n+1}}{\Delta X^2}\right)\alpha \\ & + P_{1,i}\left(\frac{(\bar{C}_i)_{j+1}^{n} - 2(\bar{C}_i)_j^{n} + (\bar{C}_i)_{j-1}^{n}}{\Delta X^2}\right)(1-\alpha) \\ & - P_{2,i}\left(\frac{(\bar{C}_i)_j^{n+1} - (\bar{C}_i)_{j-1}^{n+1}}{\Delta X}\right)\alpha \\ & - P_{2,i}\left(\frac{(\bar{C}_i)_j^{n} - (\bar{C}_i)_{j-1}^{n}}{\Delta X}\right)(1-\alpha) + (f_i)_j^{n+1}\alpha + (f_i)_j^n(1-\alpha), \end{aligned} \tag{37}$$

where j denotes the spatial position, n the time step, and α a computational constant. Iteration is required at each time step because of the nonlinearity of these equations.

4. Results and discussion

Figure 2 compares the simulated results of bioremediation computed by the present algorithm for a once-through operation in a soil bed with those obtained by Wu et al.

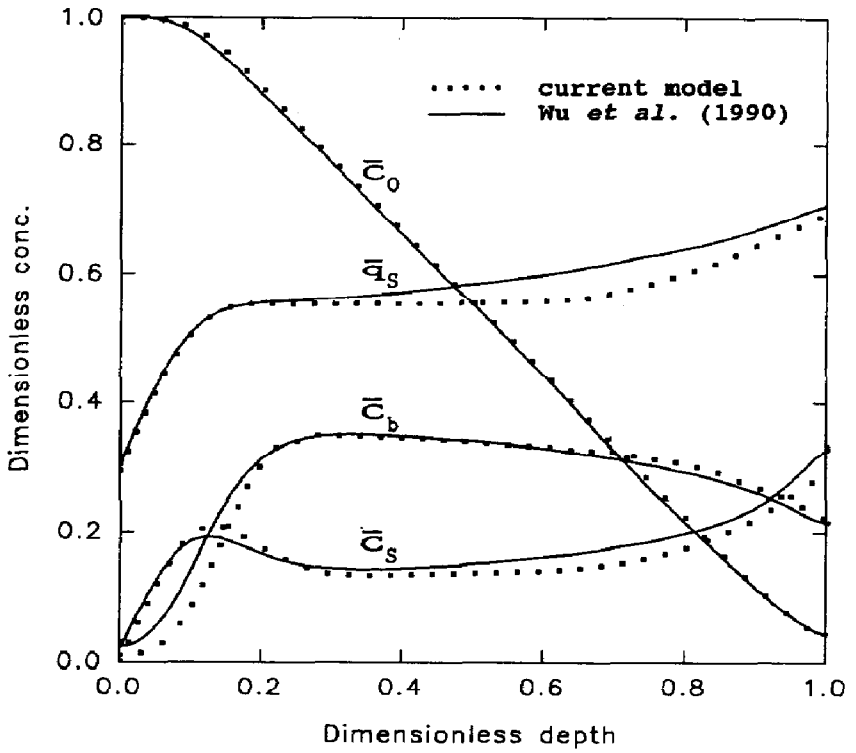

Fig. 2. Comparison between the numerical results obtained from the present model and those from the model of Wu et al. [18].

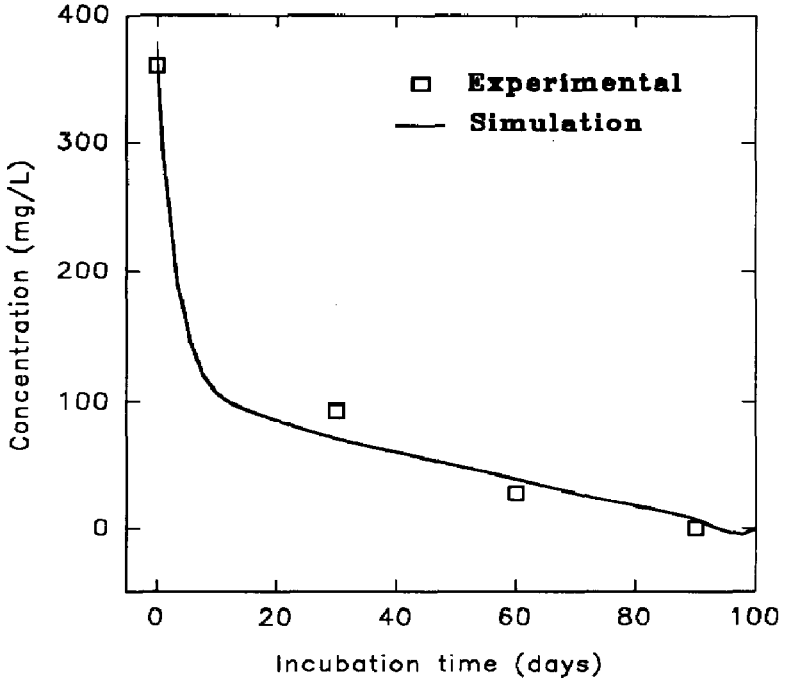

Fig. 3. Comparison of the model prediction for biodegradation of sodium palmitate at 2.0 cm depth in a 4.0 cm column with the experimental data from Tuitemwong et al. [39].

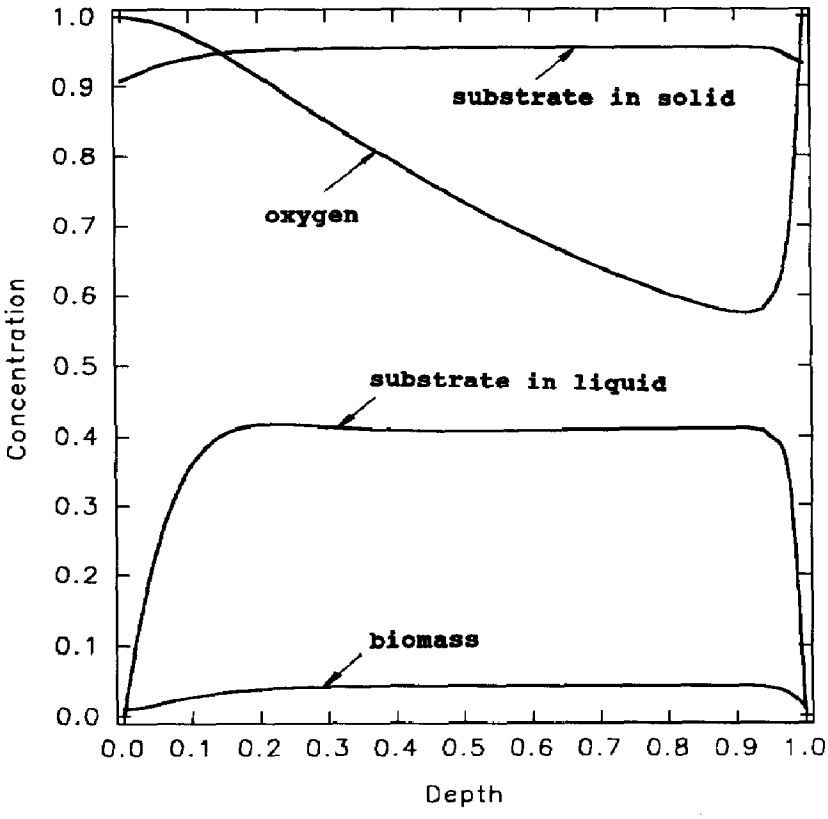

Fig. 4. Dimensionless concentration as a function of the dimensionless depth for $u = 1.0 \times 10^{-4}$ cm/s, $Pe = 100$, and $\theta = 1.0$.

Table 1
Values of parameters for numerical simulations

$a = 10^3$ cm^2/cm^3	$C_{bo} = 2.0 \times 10^{-8}$ g/cm	$C_o^* = 8.0 \times 10^{-6}$ g/cm^3
$C_{so}^* = 2.5 \times 10^{-6}$ g/cm^3	$E = 2 \times 10^{-5}$ cm^2/s	$k_d = 1.0 \times 10^{-6}$/s
$k_s = 2.0 \times 10^{-8}$ cm/s	$K_s = 7.5 \times 10^{-6}$ g/cm^3	$K_o = 4.0 \times 10^{-7}$ g/cm^3
$K_{db} = 9.3$ cm^3/g	$K_{ds} = 15$ cm^3/g	$L = 20$ cm
$u = 1.0 \times 10^{-4}$ cm/s	$q_{so} = 3.75 \times 10^{-5}$ g/g	$Y_o = 0.5$ g/g
$u = 1.0 \times 10^{-5}$ cm/s	$Y_s = 1.0$ g/g	$\mu_m = 6 \times 10^{-5}$/s
$u = 1.0 \times 10^{-6}$ cm/s	$\varepsilon = 0.3$	$\rho = 1.58$ g/cm^3

[18]. The comparison indicates that the present algorithm is capable of yielding accurate numerical results. Moreover, it has been found that the algorithm's speed of convergence is high.

The proposed model has been assessed in the light of available experimental data obtained in a soil column for biodegradation of sodium palmitate [39]. As illustrated in Fig. 3, the simulated results based on the present model are in reasonable accord with the experimental data which are single-point measurements.

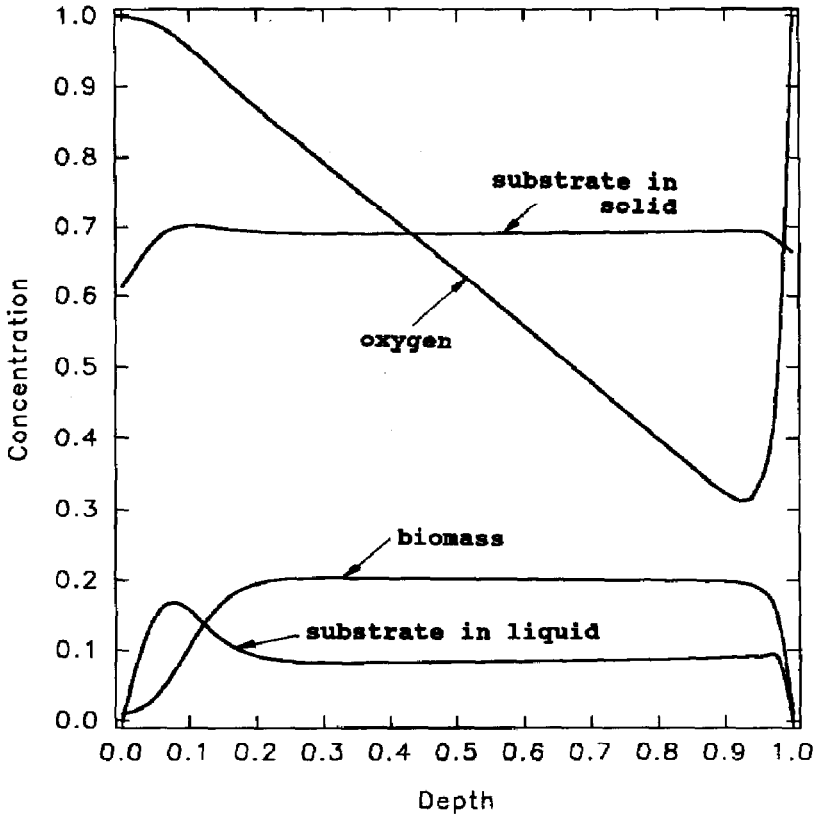

Fig. 5. Dimensionless concentration as a function of the dimensionless depth for $u = 1.0 \times 10^{-4}$ cm/s, $Pe = 100$, and $\theta = 5.0$.

Additional simulations have been performed to examine parametrically the system; the values of the parameters are listed in Table 1. The subsurface flow velocity changes from 1.0×10^{-4} to 1.0×10^{-6} cm/s, which corresponds to the soil properties varying from silt to clay for a water pressure drop caused by the natural altitude difference of the bed.

Figures 4–6 describe the variation of concentration profiles in the soil as a function of time and position for the Peclet number of 100 and the velocity of 1.0×10^{-4} cm/s. The transport processes are slow compared to the reaction rates, since the dispersion Damköhler number, $\mu_m L^2/E$, representing the ratio of the maximum depletion rate to the maximum dispersion rate is 1200, and the convection Damköhler number, $\mu_m L/u$, representing the ratio of the maximum depletion rate to the maximum convection rate is 12; both are much larger than one. The supply of oxygen by means of convection and dispersion is sufficiently rapid so that no anaerobic condition is generated.

The hydraulic conductivity in Figs. 7 and 8 is lower than that in Figs. 4–6 and the groundwater flow velocity is equal to 1.0×10^{-5} cm/s. The spatial dimensionless concentration distributions change drastically. Although the dispersion Damköhler number $\mu_m L^2/E$ remains unchanged, the convection Damköhler number $\mu_m L/u$ is now 120; this implies that the rate of transport is very low relative to the rates of the

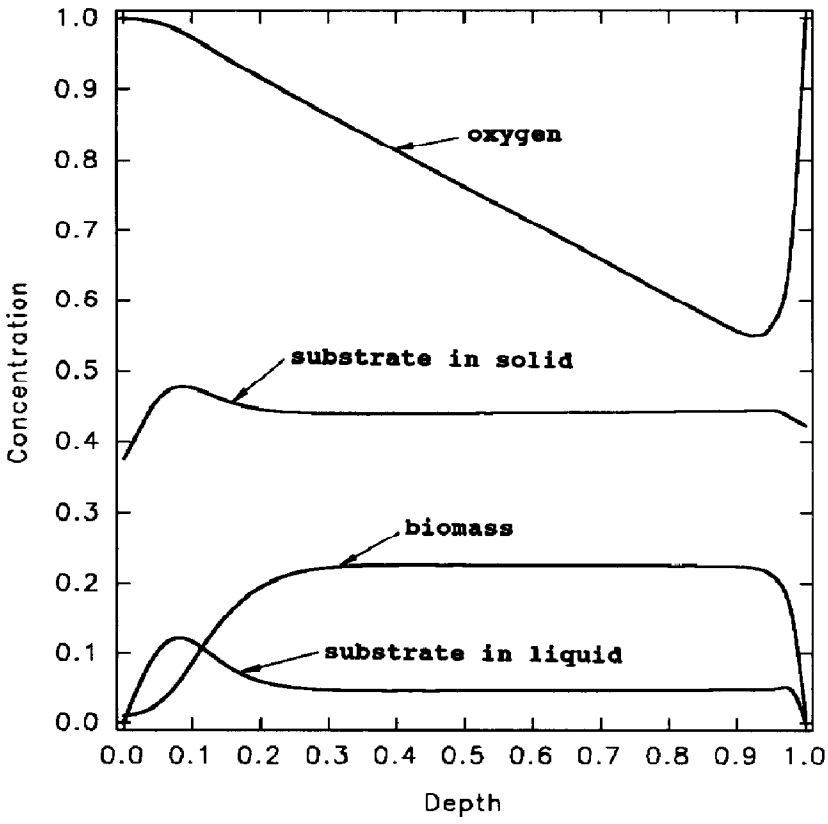

Fig. 6. Dimensionless concentration as a function of the dimensionless depth for $u = 1.0 \times 10^{-4}$ cm/s, $Pe = 100$, and $\theta = 10.0$.

reactions. An anaerobic zone is observed in the middle of the bed. Two peaks of the biomass concentration occur at the two ends where oxygen supply is sufficient. As degradation proceeds, the anaerobic zone becomes progressively smaller and eventually disappears along with the depletion of substrate (Fig. 8).

When the hydraulic conductivity is further reduced and the Peclet number approaches one, the dispersive and convective terms have the same order of magnitude in the governing equations. The simulation result is shown in Fig. 9 for $u = 1.0 \times 10^{-6}$ cm/s and $Pe = 1$. The profiles are essentially symmetric spatially, thus indicating that the dispersion is significant for the process. An anaerobic zone is present, and the desorption of the substrate from the soil particles is maintained near equilibrium.

For the limiting case in which the soil permeability approaches zero, i.e., convective flow in the soil layer vanishes, the profiles of concentration distributions are spatially symmetric, as depicted in Fig. 10. In this case, oxygen transfers only by diffusion, the rate of which limits the biotransformation inside the soil layer. Thus, the middle part of the bed is anoxic and local equilibrium is reached there.

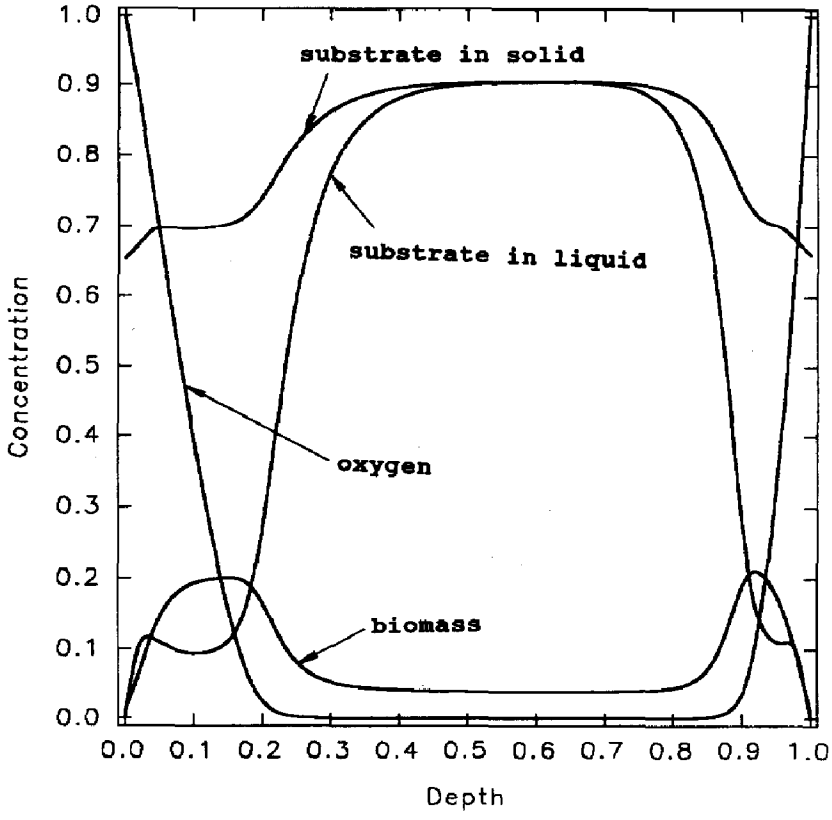

Fig. 7. Dimensionless concentration as a function of the dimensionless depth for $u = 1.0 \times 10^{-5}$ cm/s, $Pe = 10$, and $\theta = 0.5$.

To describe the extent of remediation, the concept of total organic substrate (TOS) is introduced. In the soil bed,

$$\mathrm{TOS} = \int_V \rho q_s \, \mathrm{d}V + \int_{\varepsilon V} C_s \, \mathrm{d}V. \tag{38}$$

Obviously, the TOC (total organic carbon) in the bed is equal to σTOS, where σ is the weight fraction of carbon in the organic contaminant. TOS can be normalized by dividing it by its initial value, TOS_i, as follows (see Appendix A):

$$\overline{\mathrm{TOS}} = \left(1 - \frac{1}{R_s}\right) \int_0^1 \left(\bar{q}_s + \frac{1}{R_s - 1} \bar{C}_s\right) \mathrm{d}X. \tag{39}$$

This quantity represents the fraction of residual substrate in the bed. The reacted substrate (RS), signifying the portion of substrate in the soil bed degraded by microorganisms, is defined as

$$\mathrm{RS} = \int_t \int_{\varepsilon V} \frac{\mu_m}{Y_s} R_b C_b \left(\frac{C_s}{K_s + C_s}\right)\left(\frac{C_o}{K_o + C_o}\right) \mathrm{d}V \, \mathrm{d}t, \tag{40}$$

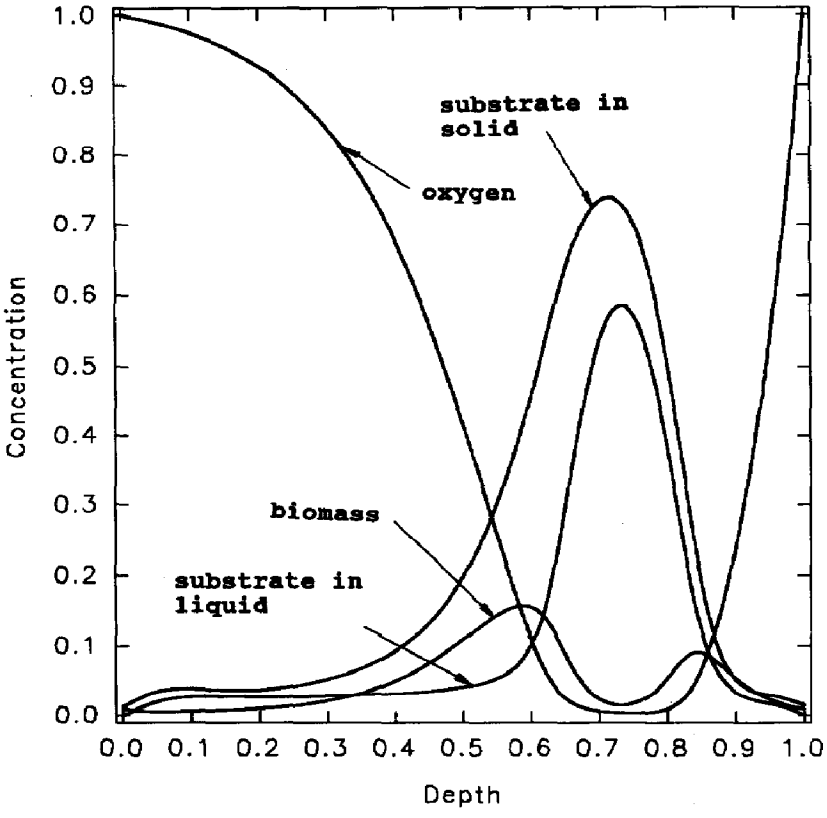

Fig. 8. Dimensionless concentration as a function of the dimensionless depth for $u = 1.0 \times 10^{-5}$ cm/s, $Pe = 10$, and $\theta = 5.0$.

which, in normal form, is

$$\overline{\mathrm{RS}} = \int_0^{\theta}\int_0^1 N_{\mathrm{r1}}\bar{C}_{\mathrm{b}}\left(\frac{\bar{C}_{\mathrm{s}}}{\bar{K}_{\mathrm{s}}+\bar{C}_{\mathrm{s}}}\right)\left(\frac{\bar{C}_{\mathrm{o}}}{\bar{K}_{\mathrm{o}}+\bar{C}_{\mathrm{o}}}\right)\mathrm{d}X\,\mathrm{d}\theta. \tag{41}$$

Thus, the fraction of substrate washed out is equal to $(1 - \overline{\mathrm{TOS}} - \overline{\mathrm{RS}})$.

The profiles of $\overline{\mathrm{TOS}}$ vs. time at different velocities, plotted in Fig. 11, reveal that the velocity of groundwater flow affects the rate of contaminant depletion; the higher the velocity, the greater the availability of oxygen and the faster the substrate consumption. Figure 12 demonstrates that the gradient of $\overline{\mathrm{TOS}}$ representing the overall substrate depletion rate decreases gradually with time. Thus, for the same quantity being removed, a much longer time is required at the end than at the beginning. Such a tailing effect is also observed in Fig. 11 at different velocities. A similar conclusion has been reported in field experiments [40]. The very slow decomposition at low contaminant concentrations usually renders the time scale of in situ bioremediation to be months or years.

The effect of water flow velocity on the time required for complete restoration ($\overline{\mathrm{TOS}} < 0.05$) is listed in Table 2. The flow velocity usually determines the remediation

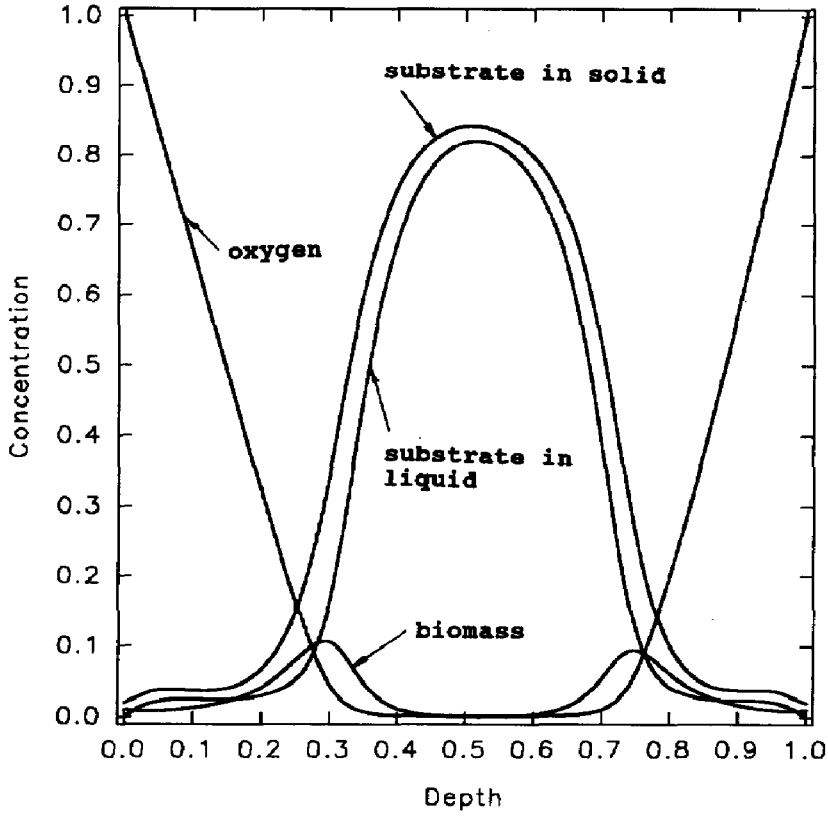

Fig. 9. Dimensionless concentration as a function of the dimensionless depth for $u = 1.0 \times 10^{-6}$ cm/s, $Pe = 1$, and $\theta = 0.5$.

time scale. When the velocity varies from 1.0×10^{-4} cm/s towards zero, the clean-up requires a time from about 3 months to almost 3 years. For these transport-limited cases, the portion of the substrate washed out is small; the major portion is transformed. If no measures are taken to remediate a contaminated site, e.g., an aquifer in the saturated zone, 14 years are required for 95% of the contaminant to diffuse out of the layer, provided that the site is biologically sterile; see case 5 in Table 2.

5. Conclusions

This paper presents a hydrochemical model consisting of coupled differential equations for describing the contaminant fate, oxygen consumption and microbial growth. Oxygen is considered to be a growth limiting factor, and nonequilibrium adsorption–desorption of the contaminant is assumed between phases. As the hydraulic conductivity varies from that of silt to that of homogeneous clay, the pattern of bioremediation changes significantly. The simulated overall depletion of the contaminant reveals that the higher the velocity of the groundwater flow, the faster the

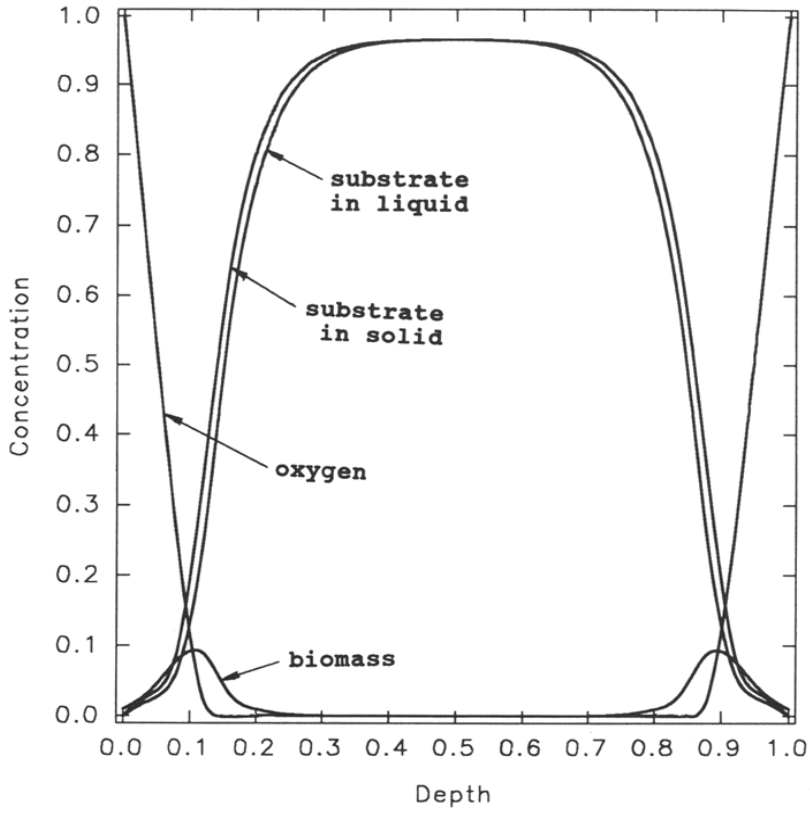

Fig. 10. Dimensionless concentration as a function of the dimensionless depth for $u = 0.0$ cm/s, and $t = 30$ days.

decrease in the contaminant concentration. At low permeability such as that encountered in groundwater flow through clay, an anaerobic zone may be generated, thereby reducing the biotransformation rate and prolonging the remediation time.

The contaminant in the low-flow or nonflow zone is often a continual source of pollution. Heterogeneous soil formation greatly hinders the effort of groundwater treatment and soil remediation. The remediation in the low permeability region of the soil usually determines the time scale of restoration.

Acknowledgment

Although the research described in this article has been funded in part by the United States Environmental Protection Agency under assistance agreement R-815709 to the Great Plains-Rocky Mountain Hazardous Substance Research Center for US EPA Regions 7 and 8 with headquarters at Kansas State University, it has not been subjected to the Agency's peer and administrative review and therefore may not necessarily reflect the views of the agency and no official endorsement should be inferred. This research was partially supported by the Kansas State University Center for Hazardous Substance Research.

Nomenclature

a	interfacial area of the aqueous and solid phases per unit volume of the soil bed, L^2/L^3
A	actual flux area of the chambers, L^2
C	concentration in the aqueous phase, M/L^3
C_{b0}	initial concentration of biomass, M/L^3
C_i^f	feed concentrations, M/L^3
C_o^s	air–water saturated concentration of oxygen, M/L^3
C_{s0}^*	concentration of substrate in the liquid phase in equilibrium with q_{s0}, M/L^3
E	dispersive coefficient, L^2/t
F_α, F_β, F_3	flow rate, L^3/t
G_i	mass generation rate of ith species per unit aqueous volume, $M/(L^3\,t)$
k_d	decay rate constant, t^{-1}
K_{db}	partition coefficient of biomass
K_{ds}	partition coefficient of substrate
K_o	saturation constant of oxygen, M/L^3
k_s	mass transfer coefficient of substrate
K_s	saturation constant of substrate, M/L^3
L	depth of the soil bed, L
q	concentration in solid aggregates, M/L^3
q_s^*	concentration of substrate in solid particles in equilibrium with that in the mobile aqueous phase, M/L^3
q_{s0}	initial concentration of substrate in solid particles, M/L^3
R_b	retardation factor of biomass $(=1+\rho K_{db}/\varepsilon)$
r_i	reaction rate, $M/(L^3\,t)$
R_s	retardation factor of substrate $(=1+\rho K_{ds}/\varepsilon)$
t	time, t
u	mean pore water velocity in the chambers, L/t
V	aqueous volumes of the chambers, L^3
x	axis, L
Y	yield factors, M/M

Greek letters

α	computational constant
δ	width of the interfacial control volume, L
ε	void fraction of the soil
μ_m	maximum specific growth rate of biomass, t^{-1}
ρ	bulk density of the soil bed, M/L^3
σ	weight fraction of carbon in a molecule

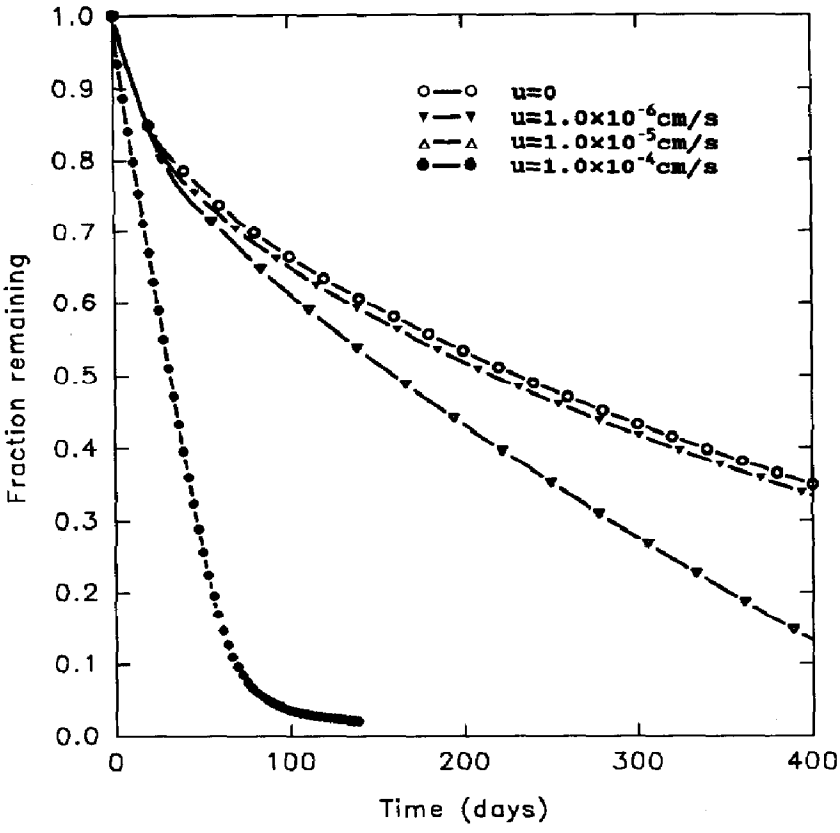

Fig. 11. Comparison of the overall fraction of substrate remaining, $\overline{TOS}$ for different groundwater flow velocities.

Subscript

b	biomass
i	*i*th species
j	spatial position in the numerical scheme
o	oxygen
s	substrate
1	upper chamber
2	soil bed
3	lower chamber

Superscript

f	quantities in the feed
n	time step in the numerical scheme
–	represents dimensionless or normalized variables

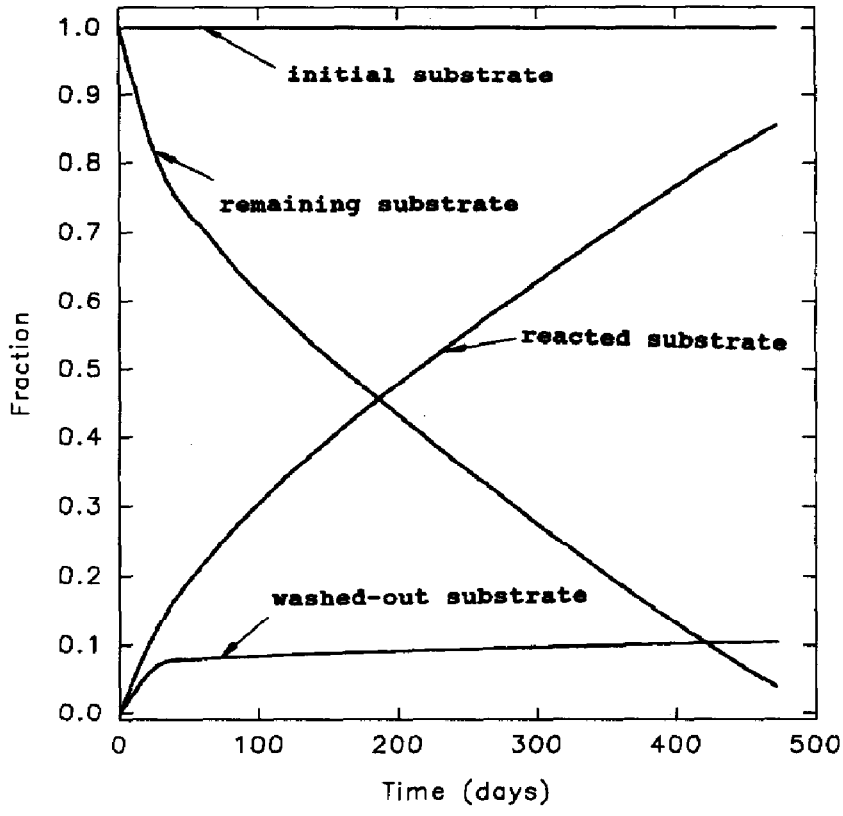

Fig. 12. Fate of substrate in the bed for $u = 1.0 \times 10^{-5}$ cm/s and $Pe = 10$.

Appendix A: Derivation of $\overline{\text{TOS}}$ and $\overline{\text{RS}}$

For a one-dimensional system, Eq. (38) can be written as

$$\text{TOS} = \int_0^L \rho q_s \, dx + \int_0^L \varepsilon C_s \, dx. \tag{A.1}$$

Because of (21), the initial TOS, TOS_i, is

$$\text{TOS}_i = \int_0^L \rho q_{s0} \, dx + \int_0^L \varepsilon C_{s0}^* \, dx = \int_0^L \left(\rho q_{s0} + \frac{\varepsilon q_{s0}}{K_{ds}} \right) dx \tag{A.2}$$

$$= \frac{R_s}{R_s - 1} \rho q_{s0} L.$$

Dividing (A.1) by this equation and combining the resultant expression with (22) and (34) give:

$$\overline{\text{TOS}} = \left(1 - \frac{1}{R_s} \right) \int_0^1 \left(\bar{q}_s + \frac{1}{R_s - 1} \bar{C}_s \right) dX. \tag{A.3}$$

Table 2
Effect of groundwater flow velocity on the time required for completion of the remediation process

Case No.	1	2	3	4	5[a]
Flow velocity, cm/s	1.0×10^{-4}	1.0×10^{-5}	1.0×10^{-6}	0.	0.
Remediation time, days	86	472	880	920	5260
Substrate remaining, %	4.96	3.94	4.83	4.37	4.95
Substrate reacted, %	69.86	85.63	85.35	86.74	0.
Substrate washed out, %	25.18	10.43	9.82	8.89	95.05

[a] No biodegradation for Case 5.

Similarly, (40) in the text can be written as

$$\mathrm{RS} = \int_0^t \int_0^L \varepsilon \frac{\mu_m}{Y_s} R_b C_b \left(\frac{C_s}{K_s + C_s}\right)\left(\frac{C_o}{K_o + C_o}\right) \mathrm{d}t\, \mathrm{d}x. \tag{A.4}$$

Dividing this equation by (A.2) and combining the resultant expression with (21), (22), 28), (29) and (31) yield

$$\overline{\mathrm{RS}} = \int_0^\theta \int_0^1 N_{r1} \bar{C}_b \left(\frac{\bar{C}_s}{\bar{K}_s + \bar{C}_s}\right)\left(\frac{\bar{C}_o}{\bar{K}_o + \bar{C}_o}\right) \mathrm{d}X\, \mathrm{d}\theta. \tag{A.5}$$

This is Eq. (41).

References

[1] D.R. Nielsen, M.Th. van Genuchten and J.W. Biggar, Water flow and solute transport processes in the unsaturated zone, Water Resource Res., 22 (1986) 89S–108S.

[2] P.S.C. Rao, D.E. Rolston, R.E. Jessup and J.M. Davidson, Solute transport in aggregated porous media: Theoretical and experimental evaluation, Soil Sci. Soc. Am. J., 44 (1980) 1139–1146.

[3] K.M. Scow and M. Alexander, Effect of diffusion on the kinetics of biodegradation: Experimental results with synthetic aggregates, SSSA J., 56 (1992) 128–134.

[4] S. Dhawan, L.E. Erickson and L.T. Fan, Model development and simulation of bioremediation in soil beds with aggregates, Ground Water, 31 (1993) 271–284.

[5] K.J. Beven, Modeling preferential flow: An uncertain future? In: T.J. Gish and A. Shirmohammadi (Eds.), Preferential Flow, ASAE, St. Joseph, MI, 1991, pp. 1–11.

[6] J.C.S. Long, J.S. Remer, C.R. Wilson, J.R. Jones and P.A. Witherspoon, Porous media equivalents for networks of discontinuous fractures, Water Resource Res., 18 (1982) 645–658.

[7] U. Hornung and R.E. Showalter, Diffusion models for fractured media, J. Math. Anal. Appl., 147 (1990) 69–80.

[8] H.H. Gerke and M.T. van Genuchten, A dual-porosity model for simulating the preferential movement of water and solutes in structured porous media, Water Resource Res., 29 (1993) 305–319.

[9] W.M. Edwards, R.R. van der Ploeg and W. Ehlers, A numerical study of the effects of non-capillary size pores upon infiltration, Soil Sci. Soc. Am. J., 43 (1979) 851–856.

[10] K.J. Beven and P. Germann, Water flow in soil macropores, II, a combined flow model, J. Soil Sci., 32 (1981) 15–29.

[11] J.S.Y. Wang and T.N. Narasimhan, Hydrologic mechanisms governing fluid flow in a partially saturated fractured, porous media, Water Resource Res., 21 (1985) 1861–1874.
[12] A.C. Bruggeman and S. Mostaghimi, Simulation of preferential flow and solute transport using an efficient finite element model, In: T.J. Gish and A. Shirmohammadi (Eds.), Preferential Flow, ASAE, St. Joseph, MI, 1991, pp. 244–255.
[13] F.T. Molz, M.A. Widdowson and L.D. Benefield, Simulation of microbial growth dynamics coupled to nutrient and oxygen transport in porous media, Water Resource Res., 22 (1986) 1207–1216.
[14] W.J. Grenney, C.L. Caupp, R.C. Sims and T.E. Short, A mathematical model for the fate of hazardous substances in soil: Model description and experimental results, Hazardous Waste and Hazardous Mater., 4 (1987) 223–239.
[15] B.D. Symons, R.C. Sims and W.J. Grenney, Fate and transport of organics in soil: Model predictions and experimental results, J. Water Pollut. Control Fed., 60 (1988) 1684–1693.
[16] T.C. Harmon, W.P. Ball and P.V. Roberts, Nonequilibrium transport of organic contaminants in groundwater, reactions and movement of organic chemicals in soils, In: B.L. Sawhney and K. Brown (Eds.), SSSA special publication number 22, Madison, WI, 1989, pp. 405–437.
[17] J.S. Kindred and M.A. Celia, Contaminant transport and biodegradation 2. Conceptual model and test simulations, Water Resource Res., 25 (1989) 1149–1159.
[18] J.C. Wu, L.T. Fan and L.E. Erickson, Modeling and simulation of bioremediation of contaminated soil, Environ. Progress, 9 (1990) 47–56.
[19] Y. Chen, L.M. Abriola, P.J.J. Alvarez, P.J. Anid and T.M. Vogel, Modeling transport and biodegradation of benzene and toluene in sandy aquifer material: Comparisons with experimental measurements, Water Resource Res., 28 (1992) 1833–1847.
[20] S. Dhawan, L.T. Fan, L.E. Erickson and P. Tuitemwong, Modeling, analysis, and simulation of bioremediation of soil aggregates, Environ. Progress, 10 (1991) 251–260.
[21] G. Chung, B.J. McCoy and K.M. Scow, Criteria to assess when biodegradation is kinetically limited by intraparticle diffusion and sorption, Biotechnol. Bioeng., 41 (1993) 625–632.
[22] E.L. Cussler, Diffusion, Cambridge Univ. Press, New York, 1984, pp. 98–99.
[23] M. Silverman and M.I. Simon, Bacterial flagella, Annu. Rev. Microbiol., 31 (1977) 397–419.
[24] G. Matthess, A. Pekdeger and J. Schroeter, Persistence and transport of bacteria and viruses in groundwater – A conceptual evaluation, J. Contaminant Hydrol., 2 (1988) 171–188.
[25] P. Baveye and A. Valocchi, An evaluation of mathematical models of the transport of biologically reacting solutes in saturated soils and aquifers, Water Resource Res., 25 (1989) 1413–1421.
[26] G. McKay, S. McKee and H.R.J. Walters, Solid–liquid adsorption based on external mass transfer, macropore and micropore diffusion, Chem. Eng. Sci., 42 (1987) 1145–1151.
[27] N.H. Baek, L.S. Clesceri and N.L. Clesceri, Modeling of enhanced biodegradation in unsaturated soil zone, J. Environ. Eng., 115 (1989) 150–172.
[28] R.J. Valo, M.M. Haggblom and M.S. Salkinoja-Salomen, Bioremediation of chlorophenol containing simulated groundwater by immobilized bacteria, Water Res., 24 (1990) 253–258.
[29] S. Notodarmojo, G.E. Ho, W.D. Scott and G.B. Davis, Modelling phosphorus transport in soils and groundwater with two-consecutive reactions, Water Res., 25 (1991) 1205–1216.
[30] X. Yang, L.E. Erickson and L.T. Fan, Dispersive-convective transport in the bioremediation of contaminated clay layers, In: L.E. Erickson (Ed.), Proc. Conf. of Hazardous Waste Research, Manhattan, KS, 1992, pp. 581–599.
[31] M.L. Rochkind-Dubinsky, G.S. Sayler and J.W. Blackburn, Microbiological Decomposition of Chlorinated Aromatic Compounds, Marcel Dekker, New York, 1987, pp. 48–185.
[32] M. Alexander, Biodegradation of chemicals of environmental concern, Science, 211 (1989) 132–138.
[33] L.T. Fan, R.P. Krishnan and S.H. Lin, Mathematical modelling of aquatic systems, In: A.S. Mujumdar and R.A. Mashelkar (Eds.), Advances in Transport Processes, Vol. II, Wiley Eastern Limited, New Delhi, 1981, pp. 1–42.
[34] C.C. Travis and E.C. Etnier, A survey of sorption relationships for reactive solutes in soil, J. Environ. Qual., 10 (1981) 8–17.
[35] J.C. Parker and A.J. Valocchi, Constraints on the validity of equilibrium and first-order kinetic transport models in structured soils, Water Resource Res., 22 (1986) 399–407.

[36] W.P. Ball and P.V. Roberts, Long-term sorption of halogenated organic chemicals by aquifer material, 2. Intraparticle diffusion, Environ. Sci. Technol., 25 (1991) 1237–1249.

[37] W.J. Weber Jr., P.M. McGinley and L.E. Katz, Sorption phenomena in subsurface systems: Concepts, models and effects on contaminant fate and transport, Wat. Res., 25 (1991) 499–528.

[38] S.V. Patankar, Numerical Heat Transfer and Fluid Flow, Hemisphere, Washington DC, 1980, pp. 82–193.

[39] P. Tuitemwong, L.E. Erickson, X. Yang and L.T. Fan, Effects of depth of a soil column on the biodegradation of palmitate, In: L.E. Erickson (Ed.), Proc. Conf. of Hazardous Waste Research, Manhattan, KS, 1992, pp. 600–615.

[40] S.R. Hutchins, W.C. Downs, J.T. Wilson, G.B. Smith, D.A. Kovacs, D.D. Fine, R.H. Douglass and D.J. Hendrix, Effect of nitrate addition on biorestoration of fuel-contaminated aquifer: Field demonstration, Groundwater, 29 (1991) 571–580.